Hindawi
Shock and Vibration
Volume 2020, Article ID 8869802, 13 pages
https://doi.org/10.1155/2020/8869802

Research Article

Multi-Input-Multi-Output Continuous Swept-Sine Vibration Test Realization by Inverse Multistep Prediction Model

Wei Zheng, Huaihai Chen, and Zhengbo Luo

State Key Laboratory of Mechanics and Control of Mechanical Structures, Nanjing University of Aeronautics and Astronautics, Nanjing 210016, China

Correspondence should be addressed to Huaihai Chen; chhnuaa@nuaa.edu.cn

Received 7 July 2020; Accepted 10 September 2020; Published 28 September 2020

Academic Editor: Amr A. Nassr

As frequency-varying sine excitations in rotating machines are always emerging during run-ups and shutdowns, the multi-input-multi-output (MIMO) swept-sine test is of utter significance in product validation. At present, swept-sine vibration tests are mostly conducted with frequency-domain methods, where drive spectra are generated and updated by frequency response function (FRF), and drive signals are then generated with sinusoid oscillators. In this paper, a time-domain approach using an inverse system method based on a multistep prediction model is developed to realize the MIMO continuous swept-sine vibration test. First, the multistep prediction model of the original system is estimated in the time domain. Then, the inverse multistep prediction model is derived. After that, this model is truncated to guarantee the robustness of the inverse system and the smoothness of the generated drive signals. At last, the proposed method is validated by a simulation example with a cantilever beam and an actual test by using a three-axis shaker. The results show that the MIMO continuous swept-sine vibration test can be operated effectively by the proposed method.

1. Introduction

Rotating machines employed in helicopters, propeller-driven airplanes, washing machines, and so on constantly produce swept-sine excitations to the whole structures during their run-ups and shutdowns. The vibrations induced by swept-sine excitations must be taken into consideration for the safety and the durability of the affected structures [1]. Besides, the swept-sine test is also required in some standard during product development [2] and is often utilized in modal analysis and other experimental practices [3]. It is worth noting that the swept-sine test, as it oftentimes produces cleaner frequency response function (FRF) than the random test, is frequently performed in aircraft ground vibration tests [4, 5]. For better simulation of complex cases such as aircraft with multiple propellers, a number of methods for the multi-input-multi-output (MIMO) test, including the MIMO swept-sine test, are introduced and developed during the last decades [6–8].

The MIMO swept-sine test applies frequency-varying sinusoid excitations upon a test article and controls the response spectra at certain points to be within the acceptable limits. As a simplified substitution for the MIMO swept-sine test, the MIMO stepped-sine test is sometimes used in literatures [9, 10] and is often included in commercial vibration controllers. In the MIMO stepped-sine test, the frequency does not vary smoothly but instead steps through a sequence of fixed frequencies. In each step, the controlled responses should be pure sine signals with predetermined cycles. Therefore, discontinuities will occur when the frequency jumps between any two successive steps. This discontinuity can be mitigated but cannot be completely removed by some smoothing techniques [10, 11]. In fact, the stepped-sine test is essentially replacing sweeping process with multiple steady-state sinusoidal tests, which is not really the continuous swept-sine test. Several other frequency-domain methods for the MIMO swept-sine test were given in the literatures. A patented frequency-domain control method with the tracking filters for the sine test was proposed by Underwood [6], where

the controlled response is achieved through iterations between learning and control loops. Yin et al. [12] presented an offline swept-sine control method, which generated drive signals by the inverse of frequency response function (FRF), and the drive signals were updated according to the errors in every control loop where the error spectra were obtained by fast Fourier transform (FFT). However, applying FFT to swept-sine signals might introduce some distortions at the beginning and end of the spectra as mentioned in the literature [9]. Besides, Fourier transform is more suitable for processing steady-state signals rather than nonstationary data such as continuous MIMO swept-sine responses.

It is noted that the FRF is needed in these frequency-domain methods to connect the input and the output. However, theoretically this relationship is based on the assumption that both the input and output are of the same fixed frequency and in steady state. As this assumption is no longer valid in the swept-sine test, the relationship between the input and output should not be constructed by FRF in the frequency domain.

Hence, it seems more reasonable to control the swept-sine test by the time-domain method, even though the frequency-domain methods had been successfully used for years in engineering. There seems to be no examples of the MIMO swept-sine test controlled by the time-domain method in the existing literature, to the best of the authors' knowledge.

Among time-domain approaches, the inverse system method is suitable to solve the problem at hand, as it directly takes the targeted system responses as its input to generate drive signals. This type of method is initially developed and applied in the force estimation area. As a typical inverse system method, the inverse structure filter (ISF) which utilized the inverse of the original system's state-space model was introduced by Kammer and Steltzner [13, 14]. However, as mentioned in the literature [15], the inverse system created by the ISF is likely to be unstable, which might restrain its practicability. Regarding these disadvantages, a delayed multistep ISF method was proposed by Allen and Carne. They observed that their method could produce more stable inverse systems, though they did not prove it theoretically [15, 16]. Mao et al. [17] presented a time-domain force estimation method based on Markov parameter precise computation, and a regularization technique was utilized to deal with the ill-posed problem.

Naturally, using the inverse system for drive signals generation in the vibration test is different from force estimation, where forces are estimated in a relatively short period of time as in most of the studies mentioned previously. Several recent studies on the MIMO random test conducted by Chen et al. [18] and Zheng et al. [19, 20] have taken advantage of inverse system methods. However, drive signals for random vibration are generated and smoothed in a frame-by-frame manner, and hence the initial state at each frame can be ignored, which is not the case in the swept-sine vibration test. So, the inverse system methods developed for the random vibration test cannot be used in the swept-sine vibration test directly. To address this issue, an inverse system method is developed for the MIMO swept-sine vibration test.

The main contents of the paper are arranged as follows. In Section 2, basic formulae for the swept-sine, multistep prediction model and some other background theories are reviewed. After that, an inverse multistep prediction model is proposed, and its application in the MIMO swept-sine test is studied. In Section 3, a numerical example of the MIMO swept-sine test by a cantilever beam is demonstrated. In Section 4, the proposed method is further validated by a test with a 3-axis shaker.

2. MIMO Swept-Sine Test Method

2.1. Theoretical Background

2.1.1. Swept Sine. The MIMO swept-sine vibration test imparts frequency-varying sinusoid excitations upon a test article and controls the response spectra at certain points. At these control points, response signals should match the predefined reference swept-sine signals with some tolerable errors within the given margins.

These reference swept-sine signals are given in the form of envelope $A(t)$ and transient phase $\varphi(t)$ as shown in equation (1), which are controlled by parameters such as starting frequency (F_1), ending frequency (F_2), sweep mode (linear or logarithm), and sweep rate $(\alpha$ or $\beta)$ or sweep duration (T).

$$p(t) = A(t)\sin\varphi(t). \tag{1}$$

The change rate of phase $\varphi(t)$ is the instant circular frequency $\omega(t)$:

$$\dot{\varphi}(t) = \omega(t) = 2\pi f(t), \tag{2}$$

where $f(t)$ is the instant frequency in Hz. How this frequency varies is determined by the sweep mode.

$$f(t) = \begin{cases} F_1 + \alpha t, & \text{(linear sweep)}, \\ F_1 2^{(\beta t/60)}, & \text{(logarithmic sweep)}, \end{cases} \tag{3}$$

where $\alpha = ((F_2 - F_1)/T)$ is the linear sweep rate in Hz/s and $\beta = 60\log_2((F_2/F_1)/T)$ is the logarithmic sweep rate in oct/min. Substituting equation (3) into equation (2) and integrating the latter with zero condition yields

$$\varphi(t) = \begin{cases} 2\pi\left(F_1 t + \dfrac{1}{2}\alpha t^2\right) & \text{(linear sweep)}, \\ 2\pi\dfrac{60F_1}{\beta\ln 2}\left(2^{\beta t/60} - 1\right) & \text{(logarithmic sweep)}. \end{cases} \tag{4}$$

For the MIMO swept-sine vibration test, the amplitude A and the initial phase Φ for a certain frequency are defined in the reference spectra. Since the instant frequency is determined at any given time as shown in equation (3), both the amplitude A and the initial phase Φ are also functions of t. So, the reference signal of the ith control point can be obtained by

$$p_i(t) = A_i(t)\sin\left(\varphi(t) + \Phi_i(t)\right), \tag{5}$$

where A_i and Φ_i $(i = 1, 2, \ldots, N)$ are the ith element of A and Φ, respectively. Hence, the reference signals for the MIMO swept-sine vibration test can be written in the vector form:

$$\mathbf{p}(t) = \{A_i(t)\sin(\varphi(t) + \Phi_i(t))\}. \tag{6}$$

As mentioned in the introduction, stepped sine is often used as a simplified replacement of continuous swept sine, where a number of frequencies are defined prior to the test according to each time step t_i ($i = 0, \ldots, n-1$), with n being the number of steps. At each frequency, a fixed frequency sinusoid signal is determined by substituting t in equation (6) with t_i. However, the number of steps has a strong influence on the effectiveness of the test: if too few steps are chosen, the dynamic characteristics of the article under test might not be fully excited; too many steps, on the other hand, may cause the period for each frequency to be very brief, thus preventing the stable responses to emerge.

Therefore the stepped-sine test is flawed despite its simplicity. The key problem is that the stepped-sine test cannot achieve continuous sweep frequency and hence cannot reflect the actual continuous change process of rotating machinery. This paper focuses on solving this problem.

2.1.2. Finite Difference Model. The finite difference model is a representation of the vibration system which describes the relationship between the current responses and previous drives and responses. If we let n_i be the number of drive channels and n_o be the number of response channels, the finite difference model can be written as

$$\begin{aligned}\mathbf{y}(k) = {} & -\boldsymbol{\alpha}_1^{(0)}\mathbf{y}(k-1) - \cdots - \boldsymbol{\alpha}_p^{(0)}\mathbf{y}(k-p) + \boldsymbol{\beta}_0^{(0)}\mathbf{u}(k) \\ & + \boldsymbol{\beta}_1^{(0)}\mathbf{u}(k-1) + \cdots + \boldsymbol{\beta}_p^{(0)}\mathbf{u}(k-p),\end{aligned} \tag{7}$$

where the coefficient matrices $\alpha_i^{(0)}$ ($i = 1, \ldots, p$) of dimension $n_o \times n_o$ are associated with the $n_o \times 1$ output vectors $\mathbf{y}$ at time steps $k-1, \ldots, k-p$, while $n_o \times n_i$ matrices $\beta_i^{(0)}$ ($i = 0, 1, \ldots, p$) correspond to the $n_i \times 1$ input vectors $\mathbf{u}$ at time steps $k, k-1, \ldots, k-p$. In addition, parameter p indicates the length of time history used to predict the current responses.

2.1.3. Multistep Prediction Model. From the finite difference model, the multistep prediction model can be derived. Shifting equation (7) by one time step yields

$$\begin{aligned}\mathbf{y}(k+1) = {} & -\boldsymbol{\alpha}_1^{(0)}\mathbf{y}(k) - \cdots - \boldsymbol{\alpha}_p^{(0)}\mathbf{y}(k-p+1) + \boldsymbol{\beta}_0^{(0)}\mathbf{u}(k+1) \\ & + \boldsymbol{\beta}_1^{(0)}\mathbf{u}(k) + \cdots + \boldsymbol{\beta}_p^{(0)}\mathbf{u}(k-p+1).\end{aligned} \tag{8}$$

Substituting equation (7) into equation (8), one can obtain

$$\begin{aligned}\mathbf{y}(k+1) = {} & -\boldsymbol{\alpha}_1^{(1)}\mathbf{y}(k-1) - \cdots - \boldsymbol{\alpha}_{p-1}^{(1)}\mathbf{y}(k-p+1) \\ & - \boldsymbol{\alpha}_p^{(1)}\mathbf{y}(k-p) + \boldsymbol{\beta}_0^{(0)}\mathbf{u}(k+1) + \boldsymbol{\beta}_0^{(1)}\mathbf{u}(k) \\ & + \boldsymbol{\beta}_1^{(1)}\mathbf{u}(k-1) + \cdots + \boldsymbol{\beta}_{p-1}^{(1)}\mathbf{u}(k-p+1) \\ & + \boldsymbol{\beta}_p^{(1)}\mathbf{u}(k-p).\end{aligned} \tag{9}$$

Keep shifting and substituting equation (7) into the new one to yield

$$\begin{aligned}\mathbf{y}(k+j) = {} & -\boldsymbol{\alpha}_1^{(j)}\mathbf{y}(k-1) - \cdots - \boldsymbol{\alpha}_{p-1}^{(j)}\mathbf{y}(k-p+1) \\ & - \boldsymbol{\alpha}_p^{(j)}\mathbf{y}(k-p) + \boldsymbol{\beta}_0^{(0)}\mathbf{u}(k+j) + \boldsymbol{\beta}_0^{(1)}\mathbf{u}(k+j-1) \\ & + \cdots + \boldsymbol{\beta}_0^{(j)}\mathbf{u}(k) + \boldsymbol{\beta}_1^{(j)}\mathbf{u}(k-1) + \cdots \\ & + \boldsymbol{\beta}_{p-1}^{(j)}\mathbf{u}(k-p+1) + \boldsymbol{\beta}_p^{(j)}\mathbf{u}(k-p).\end{aligned} \tag{10}$$

The coefficient matrices can be computed by

$$\begin{aligned}\boldsymbol{\alpha}_1^{(j)} &= \boldsymbol{\alpha}_2^{(j-1)} - \boldsymbol{\alpha}_1^{(j-1)}\boldsymbol{\alpha}_1^{(0)}, \\ &\vdots \\ \boldsymbol{\alpha}_{p-1}^{(j)} &= \boldsymbol{\alpha}_p^{(j-1)} - \boldsymbol{\alpha}_1^{(j-1)}\boldsymbol{\alpha}_{p-1}^{(0)}, \\ \boldsymbol{\alpha}_p^{(j)} &= -\boldsymbol{\alpha}_1^{(j-1)}\boldsymbol{\alpha}_p^{(0)},\end{aligned} \tag{11}$$

$$\begin{aligned}\boldsymbol{\beta}_0^{(j)} &= \boldsymbol{\beta}_1^{(j-1)} - \boldsymbol{\alpha}_1^{(j-1)}\boldsymbol{\beta}_0^{(0)}, \\ &\vdots \\ \boldsymbol{\beta}_{p-1}^{(j)} &= \boldsymbol{\beta}_p^{(j-1)} - \boldsymbol{\alpha}_1^{(j-1)}\boldsymbol{\beta}_{p-1}^{(0)}, \\ \boldsymbol{\beta}_p^{(j)} &= -\boldsymbol{\alpha}_1^{(j-1)}\boldsymbol{\beta}_p^{(0)},\end{aligned} \tag{12}$$

where $j = 1, 2, \ldots, q-1$ and q represents the number of time steps of future response to be predicted. From equation (10), one can get

$$\mathbf{y}_q(k) = \mathbf{T}\mathbf{u}_q(k) + \mathbf{B}\mathbf{u}_p(k-p) - \mathbf{A}\mathbf{y}_p(k-p), \tag{13}$$

where

$$\begin{aligned}\mathbf{y}_q(k) &= \begin{bmatrix}\mathbf{y}(k) \\ \mathbf{y}(k+1) \\ \vdots \\ \mathbf{y}(k+q-1)\end{bmatrix}, \\ \mathbf{u}_q(k) &= \begin{bmatrix}\mathbf{u}(k) \\ \mathbf{u}(k+1) \\ \vdots \\ \mathbf{u}(k+q-1)\end{bmatrix},\end{aligned} \tag{14}$$

$$\begin{aligned}\mathbf{y}_p(k-p) &= \begin{bmatrix}\mathbf{y}(k-p) \\ \mathbf{y}(k-p+1) \\ \vdots \\ \mathbf{y}(k-1)\end{bmatrix}, \\ \mathbf{u}_p(k-p) &= \begin{bmatrix}\mathbf{u}(k-p) \\ \mathbf{u}(k-p+1) \\ \vdots \\ \mathbf{u}(k-1)\end{bmatrix},\end{aligned} \tag{15}$$

$$\mathbf{T} = \begin{bmatrix} \boldsymbol{\beta}_0^{(0)} & \mathbf{0} & \cdots & \mathbf{0} \\ \boldsymbol{\beta}_0^{(1)} & \boldsymbol{\beta}_0^{(0)} & \cdots & \mathbf{0} \\ \vdots & \vdots & \ddots & \vdots \\ \boldsymbol{\beta}_0^{(q-1)} & \boldsymbol{\beta}_0^{(q-2)} & \cdots & \boldsymbol{\beta}_0^{(0)} \end{bmatrix}, \tag{16}$$

$$\mathbf{A} = \begin{bmatrix} \boldsymbol{\alpha}_p^{(0)} & \boldsymbol{\alpha}_{p-1}^{(0)} & \cdots & \boldsymbol{\alpha}_1^{(0)} \\ \boldsymbol{\alpha}_p^{(1)} & \boldsymbol{\alpha}_{p-1}^{(1)} & \cdots & \boldsymbol{\alpha}_1^{(1)} \\ \vdots & \vdots & \ddots & \vdots \\ \boldsymbol{\alpha}_p^{(q-1)} & \boldsymbol{\alpha}_{p-1}^{(q-1)} & \cdots & \boldsymbol{\alpha}_1^{(q-1)} \end{bmatrix}, \tag{17}$$

$$\mathbf{B} = \begin{bmatrix} \boldsymbol{\beta}_p^{(0)} & \boldsymbol{\beta}_{p-1}^{(0)} & \cdots & \boldsymbol{\beta}_1^{(0)} \\ \boldsymbol{\beta}_p^{(1)} & \boldsymbol{\beta}_{p-1}^{(1)} & \cdots & \boldsymbol{\beta}_1^{(1)} \\ \vdots & \vdots & \ddots & \vdots \\ \boldsymbol{\beta}_p^{(q-1)} & \boldsymbol{\beta}_{p-1}^{(q-1)} & \cdots & \boldsymbol{\beta}_1^{(q-1)} \end{bmatrix}. \tag{18}$$

Equation (13) is also known as the multistep prediction model [21], which predicts future output signals from the previous input and output signals.

The initial coefficients $\alpha_i^{(0)}(i = 1, \ldots, p)$ and $\beta_i^{(0)}(i = 0, 1, \ldots, p)$ can be identified from test data. After that, $\alpha_i^{(j)}$ and $\beta_i^{(j)}$ for any j from 1 to $q-1$ can be computed using equations (11) and (12), and thus the coefficient matrices T, A, and B can be obtained by equations (16)–(18).

2.1.4. Truncated SVD. T matrix in equation (13) can be decomposed by SVD (singular value decomposition) into three matrices $\mathbf{U}, \Sigma$, and V as

$$\mathbf{T} = \mathbf{U}\boldsymbol{\Sigma}\mathbf{V}^{\mathrm{T}}, \tag{19}$$

where the left and the right matrices $\mathbf{U} \in \mathrm{R}^{qn_o \times qn_o}$ and $\mathbf{V} \in \mathrm{R}^{qn_i \times qn_i}$ are orthogonal and $\Sigma \in \mathrm{R}^{qn_o \times qn_i}$ is diagonal.

$$\boldsymbol{\Sigma} = \mathrm{diag}(\sigma_1, \sigma_2, \ldots, \sigma_k), \tag{20}$$

where $k = \min(qn_o, qn_i)$, and the singular values are arranged in a descending order:

$$\sigma_1 \geq \sigma_2 \geq \cdots \geq \sigma_k \geq 0. \tag{21}$$

For actual vibration systems, some of the singular values might be very close to zero, and the direct inverse of the T matrix might induce numerical instability, so the truncated SVD or TSVD method [22] is often used to obtain a more stable inverse. In the TSVD method, an approximation of the T matrix is produced by

$$\begin{cases} \mathbf{T}_r = \mathbf{U}\boldsymbol{\Sigma}_r\mathbf{V}^{\mathrm{T}}, \\ \boldsymbol{\Sigma}_r = \mathrm{diag}(\sigma_1, \ldots, \sigma_r, 0, \ldots, 0), \end{cases} \tag{22}$$

where r is the number of reserved singularity values which are larger than a given threshold. The pseudoinverse of $\mathbf{T}_r$ matrix can be written as

$$\begin{cases} \mathbf{T}_r^+ = \mathbf{V}\boldsymbol{\Sigma}_r^+\mathbf{U}^T, \\ \boldsymbol{\Sigma}_r^+ = \mathrm{diag}\left(\sigma_1^{-1}, \ldots, \sigma_r^{-1}, 0, \ldots, 0\right). \end{cases} \tag{23}$$

Then, $\mathbf{T}_r^+$ can be used as a pseudoinverse to preclude the ill-posed problem, and it can be seen that

$$\mathbf{T}_r^+\mathbf{T} = \begin{pmatrix} \mathbf{I}_r & \mathbf{0} \\ \mathbf{0} & \mathbf{0} \end{pmatrix}. \tag{24}$$

When using this method, the parameter r will influence the accuracy of the pseudoinverse matrix, thus affecting the result of drive signal generation. This parameter can be determined by cross validation methods [22].

2.2. A New Test Method. From the multistep prediction model of the test system, the inverse multistep prediction model can be derived and used to generate the drive signals. Combining the inverse multistep prediction model with the control strategy based on matrix power, a new time-domain MIMO sweep vibration test method can be constructed.

2.2.1. Inverse Multistep Prediction Model. If the T matrix in equation (13) were always invertible, then the inverse model could be obtained in a quite straight forward way, which is unfortunately not always true for test systems. Therefore, it is necessary to use pseudoinverse derived in equation (23) instead. Left multiply equation (13) by $\mathbf{T}_r^+$ on both sides to yield

$$\begin{aligned} \mathbf{T}_r^+\mathbf{y}_q(k) &= \mathbf{T}_r^+\mathbf{T}\mathbf{u}_q(k) + \mathbf{T}_r^+\mathbf{B}\mathbf{u}_p(k-p) - \mathbf{T}_r^+\mathbf{A}\mathbf{y}_p(k-p) \\ &= \begin{bmatrix} \mathbf{I}_r & \mathbf{0} \\ \mathbf{0} & \mathbf{0} \end{bmatrix}\mathbf{u}_q(k) + \mathbf{T}_r^+\mathbf{B}\mathbf{u}_p(k-p) - \mathbf{T}_r^+\mathbf{A}\mathbf{y}_p(k-p). \end{aligned} \tag{25}$$

It can be seen from equation (25) that only the first r elements of $\mathbf{u}_q(k)$ are selected. However, as we mentioned in equation (14), $\mathbf{u}_q(k)$ comprises drive force data from $\mathbf{u}(k)$ to $\mathbf{u}(k+q-1)$, so the first r elements might not be meaningful in practice. Therefore, in order to select the drive force data of the length l from $\mathbf{u}(k)$ to $\mathbf{u}(k+l-1)$, a new $\overline{\mathbf{T}}$ is formed by picking up the first $l \cdot n_i$ row ($l \cdot n_i < r$) of $\mathbf{T}_r^+$. Substituting $\mathbf{T}_r^+$ in equation (25) with $\overline{\mathbf{T}}$ yields a new equation:

$$\mathbf{u}_l(k) = \overline{\mathbf{T}}\mathbf{y}_q(k) + \overline{\mathbf{B}}\mathbf{y}_p(k-p) - \overline{\mathbf{A}}\mathbf{u}_p(k-p), \tag{26}$$

where $\mathbf{y}_q$, $\mathbf{y}_p$, and $\mathbf{u}_p$ are the same as in equation (14) and (15) and

$$\mathbf{u}_l(k) = \begin{bmatrix} \mathbf{u}(k) \\ \mathbf{u}(k+1) \\ \vdots \\ \mathbf{u}(k+l-1) \end{bmatrix}, \tag{27}$$

$$\begin{aligned} \overline{T} &= \begin{bmatrix} \mathbf{I}_{l \cdot n_i} & \mathbf{0} \end{bmatrix}\mathbf{T}_r^+, \\ \overline{B} &= \overline{T}\mathbf{A}, \\ \overline{A} &= \overline{T}\mathbf{B}, \end{aligned} \tag{28}$$

in which $\overline{T}$ is a $l \cdot n_i \times q \cdot n_o$ matrix, $\overline{A}$ is a $l \cdot n_i \times p \cdot n_i$ matrix, and $\overline{B}$ is a $l \cdot n_i \times p \cdot n_o$ matrix. As mentioned before, p is the number of time steps of past drives and responses and q is the number of time steps of future responses. Besides, the new parameter l stands for the time steps of future drives the inverse system generates.

Needless to say, equation (26) bears remarkable resemblance to the multistep prediction model in equation (13), except that the $\overline{T}$ matrix is truncated, which precludes the instability in the inverse system caused by the singularity problem while computing the inverse of T. Hence, the model defined in equation (26) is named as the inverse multistep prediction model hereafter and will be used in the MIMO swept-sine test.

2.2.2. Drive Signal Generation. In the real world, test articles start vibrating from rest conditions which cannot achieve stable response immediately; a segment of transient response will always exist. The reference signals for the swept-sine test actually specify the stable response of the system, so if the reference signals are used as the input for the inverse multistep prediction model directly, the drive signals generated will be unrealistic. Hence, a transition segment should be added to the forepart of the original reference signals in order to generate reasonable drive signals as illustrated in Figure 1.

To compose this transition segment, a segment of fixed frequency sine signal which matches the initial amplitude and phase of the original reference signal is generated, and a 1/4 sine window is applied to ensure the amplitude of this segment varies smoothly from zero to the same initial amplitude of the original reference signal. This transition segment is inserted before the original reference signal to modify the reference signal. Obviously, the response of this transition segment is redundant and should be ignored.

Since equation (26) produces $\mathbf{u}_l(k)$ instead of $\mathbf{u}_q(k)$, using the reference signals with a length of q can only generate drive signals with a length of l, where $l < q$. Hence, the reference signals will be used in an overlapped manner in order to generate full length drive signals. In the drive signal generating process, if the reference signals are not enough in the last segment, zeros will be supplemented. The process of drive signal generation is illustrated in Figure 2 (for clarity, the figure shows only one channel, but this process is applicable for MIMO systems).

From the above discussions, the generation of drive signals for the MIMO swept-sine test can be concluded as follows (also illustrated in Figure 3):

(a) Estimate the finite difference model of the testing system

(b) Obtain T, A, and B in equation (13) from the finite difference model

(c) Calculate the pseudoinverse of T by the TSVD method to get $\mathbf{T}_r^+$ and then to form $\overline{T}$ from $\mathbf{T}_r^+$

(d) Establish the inverse multistep prediction model as the inverse system using equation (28)

(e) Modify the reference signals and use them as the inputs of the inverse system to produce drive signals

2.2.3. Control Strategy. Due to the noises in the input and output signals and other errors in the modeling of the system, the responses of the first loop may not be satisfactory without control. An offline control strategy is put forward, in which the response spectra are obtained and compared to the reference counterparts, and thus the errors in frequency domain are obtained. Then, the reference spectra for next control loop are updated according to these errors, and the drive signals are updated afterwards. To avoid damaging the test article and equipment, it advisable to control the swept-sine responses within acceptable range at a lower level and then restore the original level test.

The reference spectra is updated as

$$\begin{cases} \mathbf{E}_n(\omega) = \left\{ \dfrac{R_0^{(i)}(\omega)}{S_y^{(i)}(\omega)} \right\}, \\ \qquad\qquad\qquad\qquad (i = 1, 2, \ldots, n_o, n = 0, 1, 2, \ldots) \\ \mathbf{R}_{n+1}(\omega) = \left\{ \left(E_n^{(i)}(\omega) \right)^{\varepsilon} R_n^{(i)}(\omega) \right\}, \end{cases} \tag{29}$$

where $\mathbf{S}_y(\omega)$ is the response spectra at present loop, $\mathbf{R}_n(\omega)$ is the reference spectra after n times of modification ($\mathbf{R}_0$ is the actual reference spectra), $\mathbf{E}_n(\omega)$ is the spectral error at present loop, $\mathbf{R}_{n+1}(\omega)$ is the modified reference spectrum for the next loop, and ε is a positive constant and $\varepsilon < 1$ [23]. All these spectra take the form of vectors, and they are used in equation (29) in an element-by-element manner, namely, $S_y^{(i)}(\omega)$, $E_n^{(i)}$, and $R_n^{(i)}(\omega)$ $(i = 1, 2, \ldots, n_o)$ represent the ith elemnt of the corresponding vectors.

The control scheme for the swept-sine test is shown in Figure 4.

3. Simulation Example

3.1. Simulation Settings. A two-input-two-output swept-sine vibration test is simulated while using an aluminum cantilever beam as the test object. The parameters of the beam are listed in Table 1 and shown in Figure 5.

The finite element model (FEM) of the cantilever beam is used in the simulation. The beam is divided evenly into 10 elements and has 20 freedoms, and all modal damping ratios are set as 0.8%. Thus, the mass (M), stiffness (K), and damping (Ξ) matrices of the system can be set up from this finite element model. The continuous state-space model of the system is

$$\begin{aligned} \dot{\mathbf{x}} &= \mathbf{A}_c \mathbf{x} + \mathbf{B}_c \mathbf{u}, \\ \mathbf{y} &= \mathbf{C}_c \mathbf{x} + \mathbf{D}_c \mathbf{u}, \end{aligned} \tag{30}$$

where $\mathbf{u}$ and $\mathbf{y}$ are the input and output vectors, $\mathbf{x}$ is the state vector, and

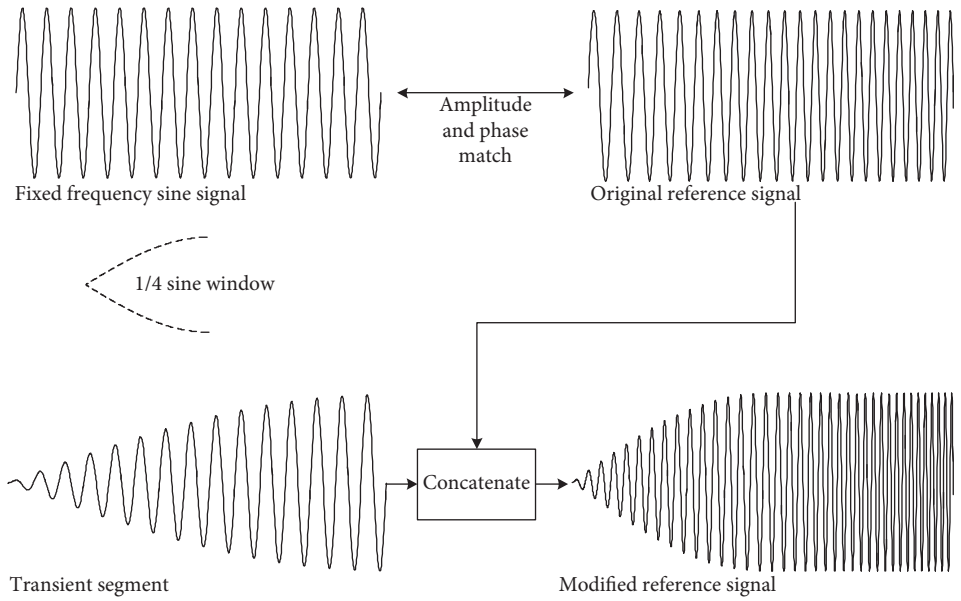

Figure 1: Modification of the original reference signal.

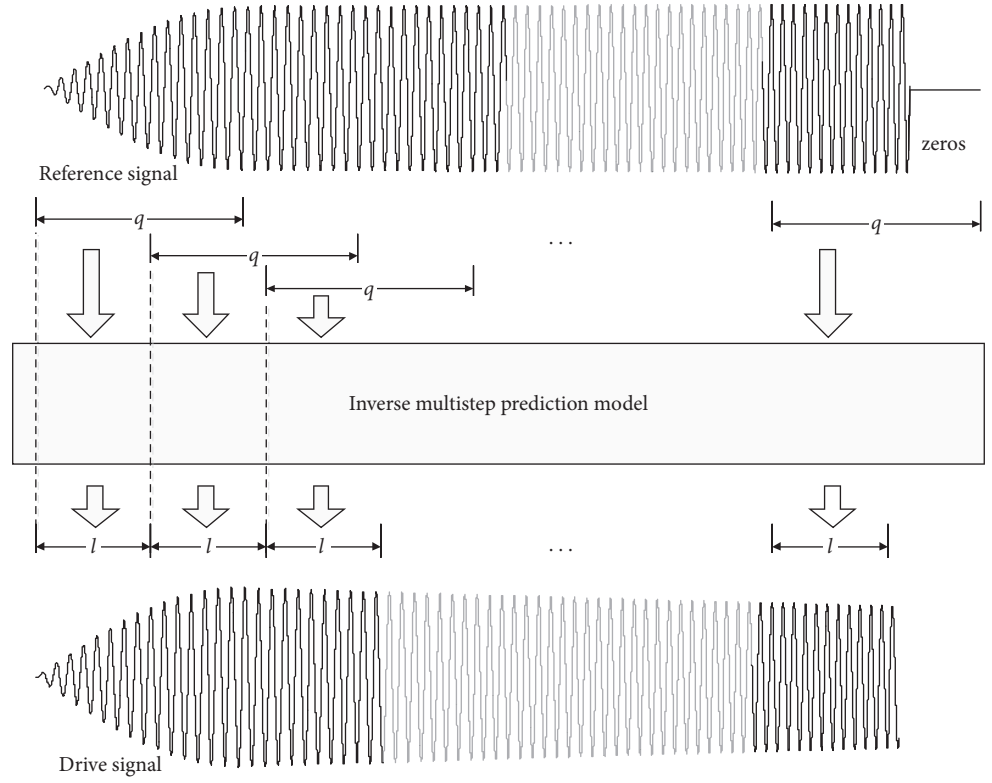

Figure 2: Drive signal is generated by the inverse system method and the reference signal is used in an overlapped manner.

$$\mathbf{A}_c = \begin{bmatrix} \mathbf{0} & \mathbf{I} \\ -\mathbf{M}^{-1}\mathbf{K} & -\mathbf{M}^{-1}\Xi \end{bmatrix},$$
$$\mathbf{B}_c = \begin{bmatrix} \mathbf{0} \\ \mathbf{M}^{-1}\mathbf{B}_f \end{bmatrix}, \quad (31)$$
$$\mathbf{C}_c = \begin{bmatrix} -\mathbf{C}_a\mathbf{M}^{-1}\mathbf{K} & -\mathbf{C}_a\mathbf{M}^{-1}\Xi \end{bmatrix},$$
$$\mathbf{D}_c = \mathbf{C}_a\mathbf{M}^{-1}\mathbf{B}_f,$$

where $\mathbf{B}_f$ is the indicating matrix used to define the excitation force on each DOF and $\mathbf{C}_a$ is used to pick up output DOFs of the state-space model. Responses can be acquired from given forces with this continuous state-space model.

In the example, the sampling frequency is 5120 Hz, the multistep prediction model of the system is estimated by a length of 1024 steps, the inverse multistep prediction model is truncated to a length of 512 steps, the sweep mode is logarithm, and the sweep speed is 2 octaves per minute (a

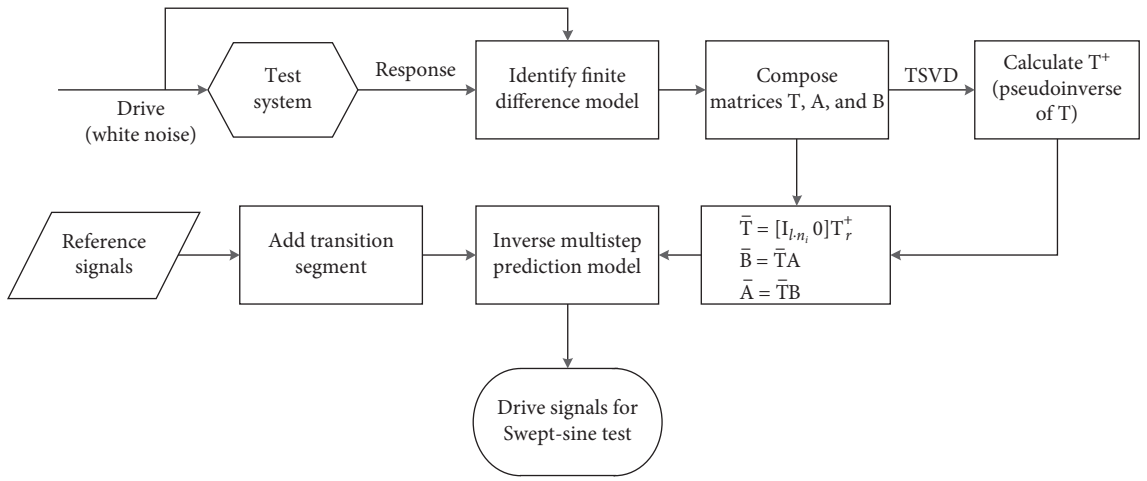

Figure 3: Generation of drive signals for the MIMO swept-sine test.

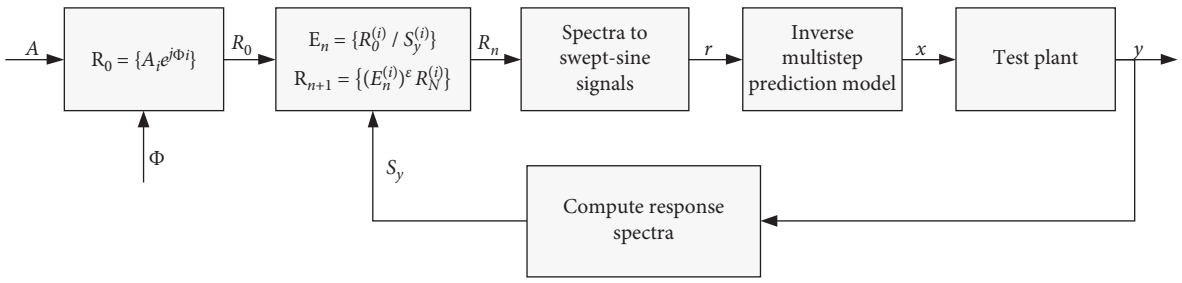

Figure 4: Offline swept-sine control scheme where A and Φ are amplitude and initial phase vectors defined in reference spectra.

Table 1: Physical properties of the beam.

Property	Value
Density (kg/m^3)	7850
Elastic modulus (MPa)	720
Length (mm)	1000
Width (mm)	50
Height (mm)	15

sweep from 5 Hz to 250 Hz takes roughly 169 seconds). The reference spectra at two control points are defined in Tables 2 and 3. The acceleration between the break points in the table is interpolated linearly on log-log axes, and the phases are formed by linear interpolation with frequency in a logarithmic scale.

In practice, the vibration at low frequency is usually given in the form of the peak-peak displacement restrictions to avoid damaging test equipment. In addition, the crossover frequency (25.73 Hz in the example) is where both requirements on acceleration and displacement are met. However, since the vibration in the test is often measured by using an accelerometer, the displacement defined in the low frequency must be transformed into acceleration. The transformation formula is

$$A = \omega^2 \frac{D}{2}, \tag{32}$$

where A represents the amplitude of acceleration and D is the peak-peak amplitude of displacement.

3.2. Simulation Results. The results of the two-input-two-output swept-sine vibration test are shown in Figure 6. Here, the amplitudes and phases of the responses at the two control points are obtained by using a Co-Quad analyzer [9].

From Figure 6, it can be seen that the amplitudes and phases of the responses at the controlled points match the references very well.

3.3. Comparison with Frequency-Domain Method. The key step in the frequency-domain methods is to get the impedance matrix by inversing the frequency response function matrix H(f) and then use it to obtain the amplitude and initial phase information of the drive signals. The calculation process is as follows:

$$\mathbf{X}(f) = \mathbf{H}^{-1}(f)\mathbf{Y}(f), \tag{33}$$

where $\mathbf{X}$ and $\mathbf{Y}$ are complex vectors. Then, the relationship between frequency and time of sweeping process $f(t)$ is substituted for $X(f)$ to obtain the amplitude $\mathbf{A}$ and initial phase Φ.

$$\begin{aligned} \mathbf{A}(t) &= \|\mathbf{X}(f(t))\|, \\ \mathbf{\Phi}(t) &= \angle(\mathbf{X}(f(t))). \end{aligned} \tag{34}$$

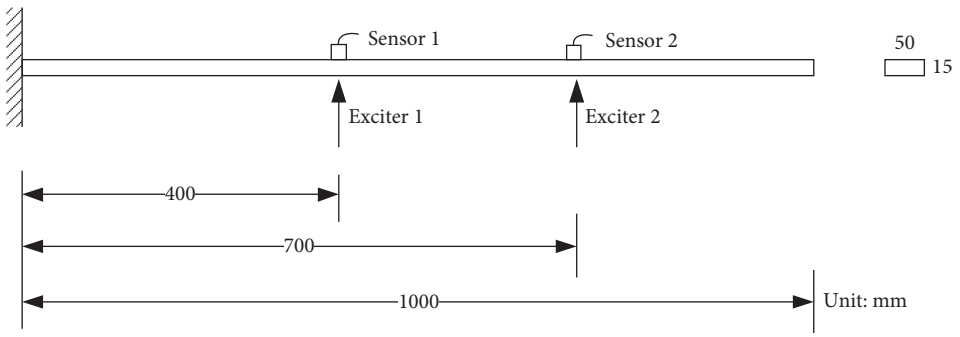

Figure 5: Cantilever beam used in simulation.

Table 2: Reference spectrum at control point 1.

	Freq. (Hz)	Acc. (g)	Disp. (mm)	Phase (°)
1	5	—	0.75	20
2	25.73	1	—	20
3	150	1	—	20
4	250	0.5	—	20

Table 3: Reference spectrum at control point 2.

	Freq. (Hz)	Acc. (g)	Disp. (mm)	Phase (°)
1	5	—	0.75	40
2	25.73	1	—	40
3	250	1	—	40

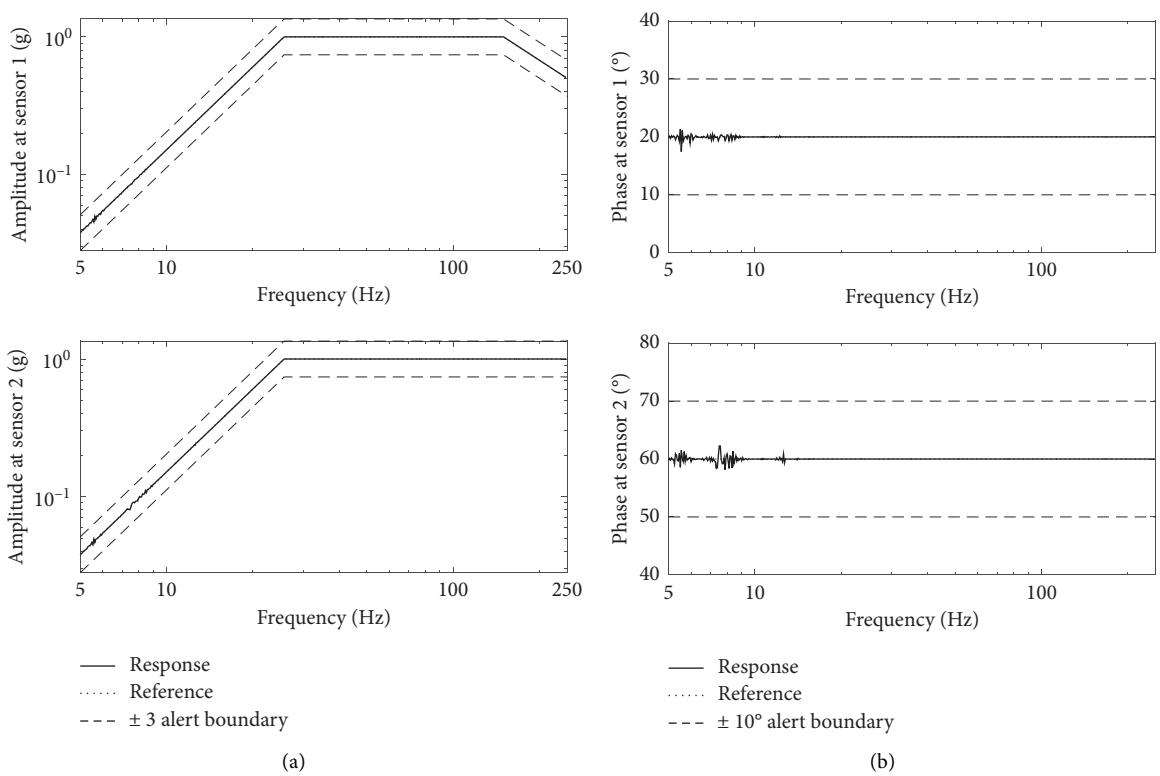

Figure 6: Simulation results of the two-input-two-output swept-sine vibration test example.

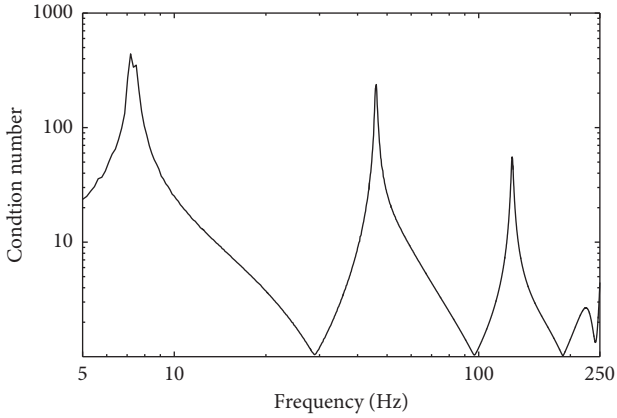

Figure 7: The condition number of FRF.

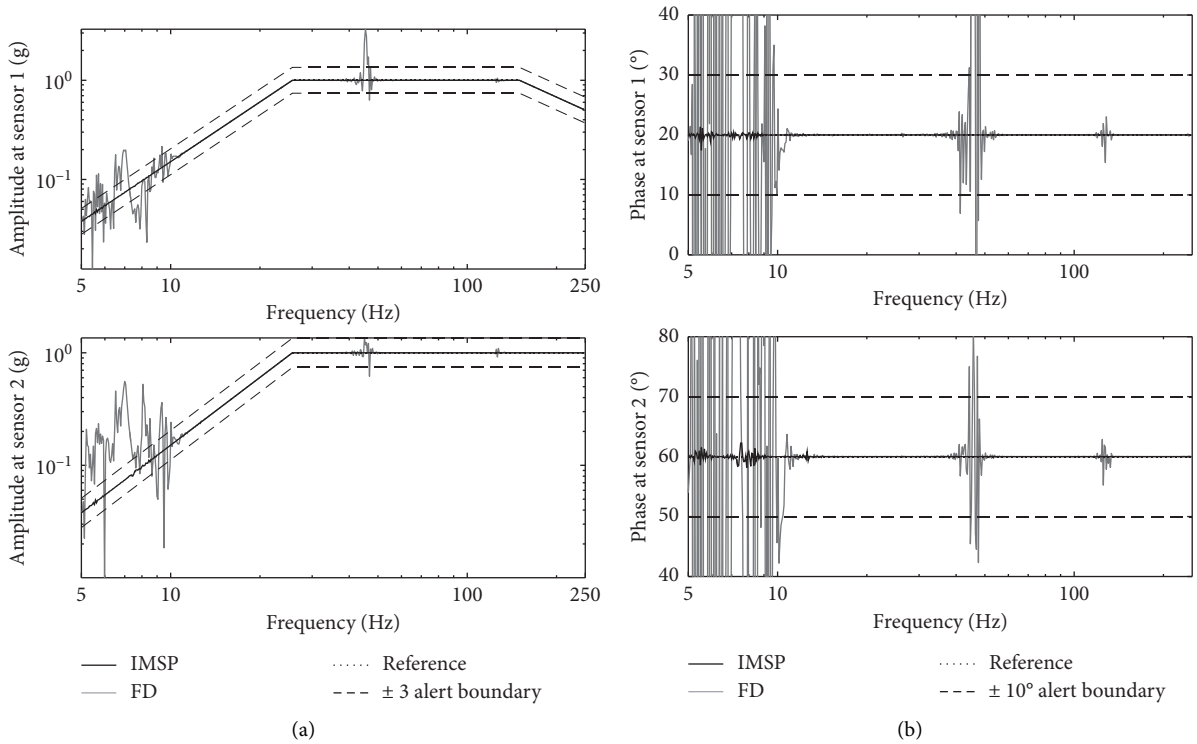

Figure 8: Comparison between the inverse multistep prediction method (IMSP) and frequency-domain method (FD).

The drive signals can be obtained by substituting the amplitude and the initial phase into equation (6). For the low damping model used in simulation, the condition number of the frequency response function matrix near the formant increases sharply, as shown in Figure 7, which makes the corresponding impedance matrix rather sensitive. Therefore, when calculating the impedance matrix, it is generally necessary to use regularization methods such as TSVD to avoid generating excessive excitation.

By comparing the inverse multistep prediction method proposed in this paper with the general frequency-domain method (Figure 8), it can be seen that the method proposed in this paper can get better results when the frequency sweeps at a rather fast rate (2 oct/min) in a low damping system. This is because the frequency response function describes the relationship between sinusoidal excitation and response in the steady state, but the sweeping process is transient and deviates from the steady-state hypothesis as the sweeping rate becomes faster. On the other hand, this issue can be avoided by the proposed method since it directly generates the drive signals according to the time-domain reference signals.

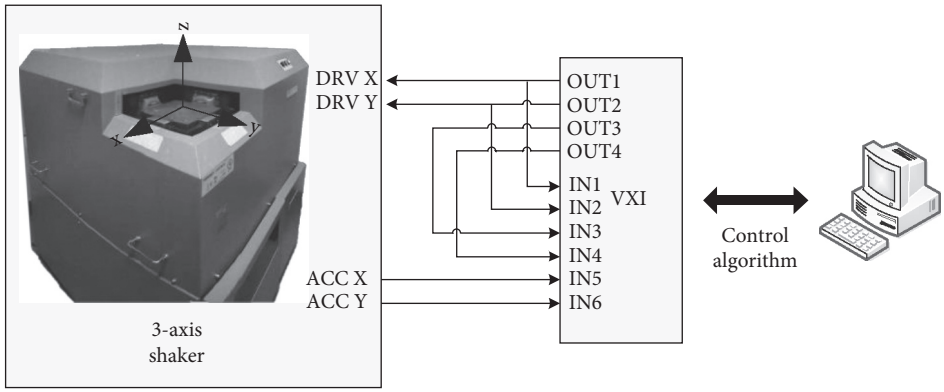

Figure 9: Test system constitution.

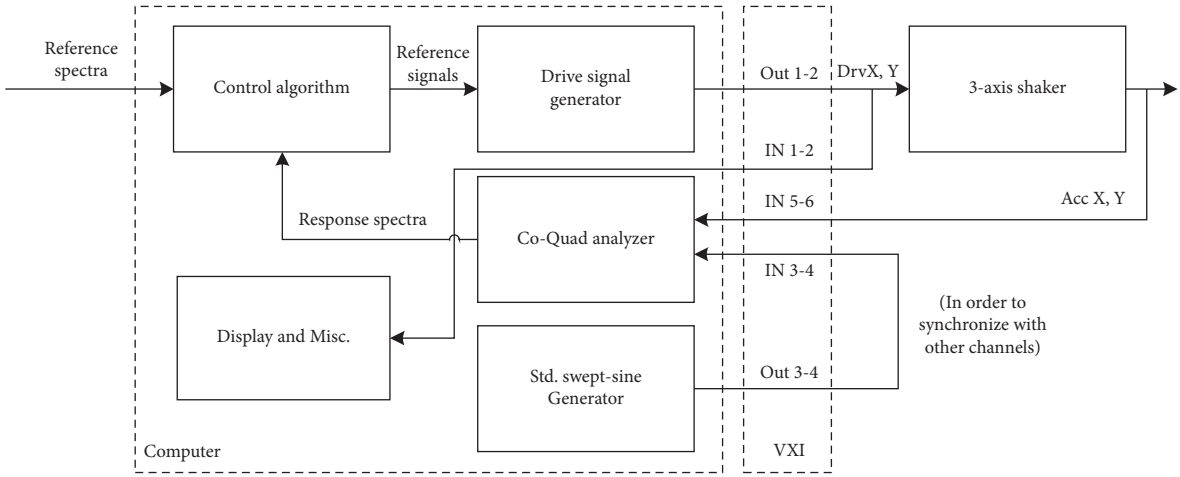

Figure 10: Block diagram for the test system.

4. Test Analysis

4.1. Test Settings. A two-input-two-output swept-sine test is conducted with a three-axis shaker to validate the method proposed in the paper. The test system exhibited in Figure 9 consists of a three-axis vibration shaker (Shinken G-6080-3HT-20), a VXI digital signal processor, two acceleration sensors, a computer, and other peripherals.

Due to the limited number of the VXI channels, only the accelerations of x and y directions of the 3-axis shaker are controlled. The VXI digital signal processor and the computer are used to form the vibration controller. In Figure 9, the first two outputs (OUT 1~2) are used as drive signal channels and the other two outputs (OUT 3~4) are used to transfer two swept-sine signals which have same amplitudes but with the phase difference of 90°. These two swept-sine signals are used as "standard signals" in order to obtain the transient frequency and to extract amplitudes and phases from responses. The first four input channels (IN 1~4) are the direct feedback from the output channels, and the last two input channels (IN 5~6) are used to acquire responses from the acceleration sensors. The roles of these inputs, outputs, and measurements are also shown in Figure 10.

The reference spectra given in the simulation example in Section 3 are used again in the test, but additional abort boundaries are set at ±6 dB. During the test, Hilbert transform [24] is applied to one of the "standard" swept-sine signals to obtain the transient frequency and amplitude. The amplitudes and phases of the responses are obtained by using a Co-Quad analyzer [9].

4.2. Test Results. A MIMO vibration test generally starts from a level lower than the normal references and climbs up to the normal reference level after it has been controlled. This is due to the fact that in MIMO cases the test cannot be controlled instantly, so in order to avoid any possible damage to the equipment, a preliminary test at a lower level is necessary. In this test, the preliminary test is conducted at the −6 dB level of the references. After 4 iteration loops, the response spectra are controlled within acceptable tolerances, and then the normal level test can be performed. The response spectra before and after control in the lower level test are shown in Figures 11 and 12, respectively. The responses in the normal level test are given in Figure 13. From Figure 11, it can be seen that the response amplitudes are roughly within the limits except for the low frequencies, but

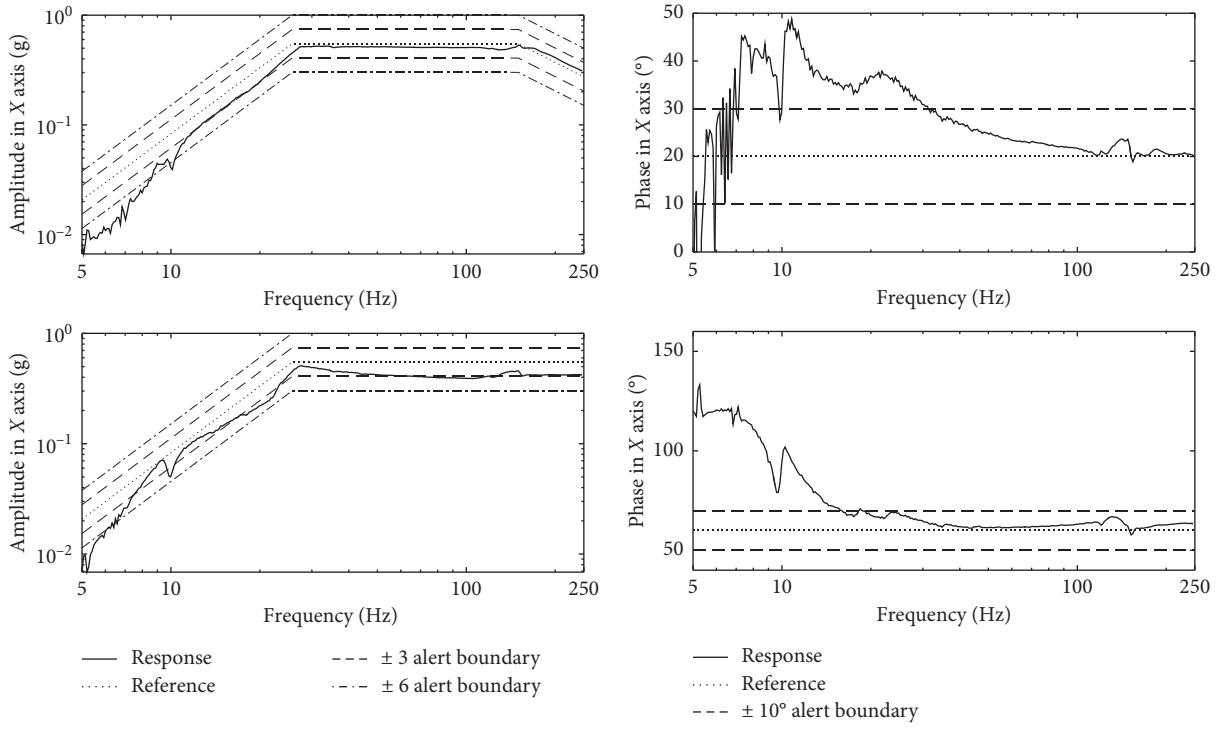

Figure 11: Responses of the lower level (−6 dB) preliminary test without control.

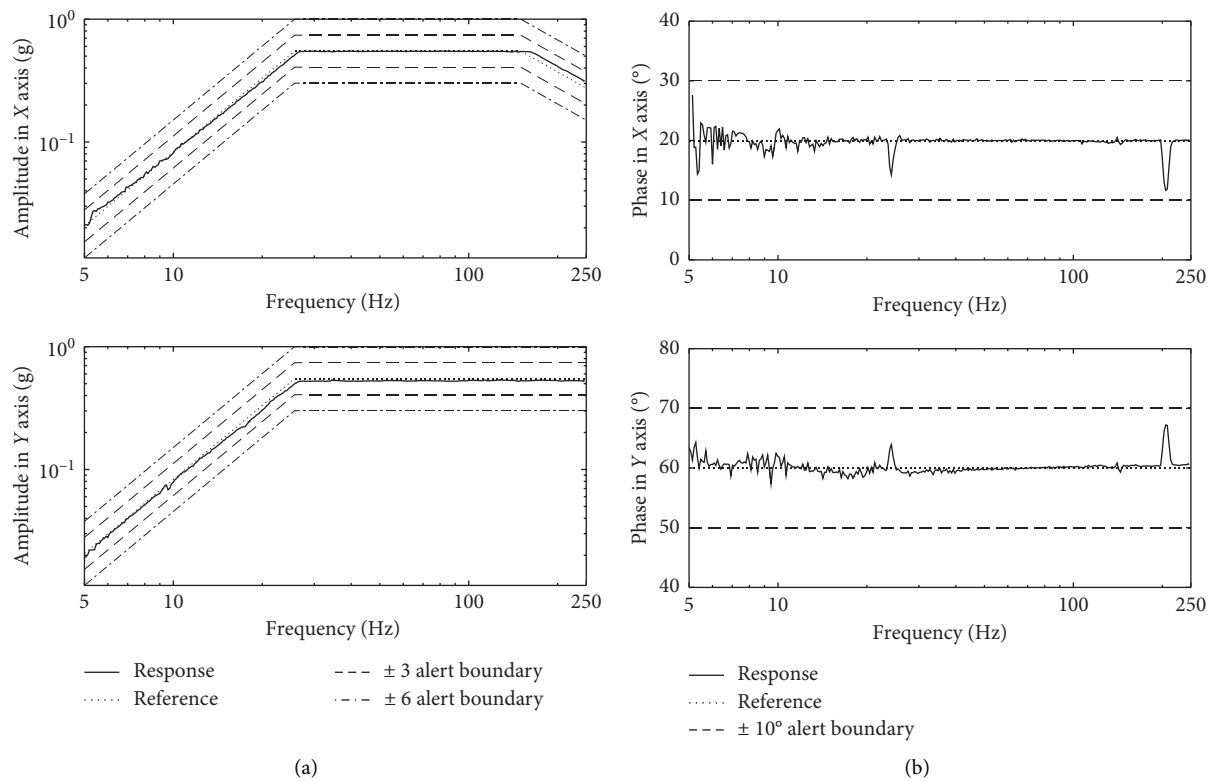

Figure 12: Responses of the lower level (−6 dB) preliminary test after control (4 iterations).

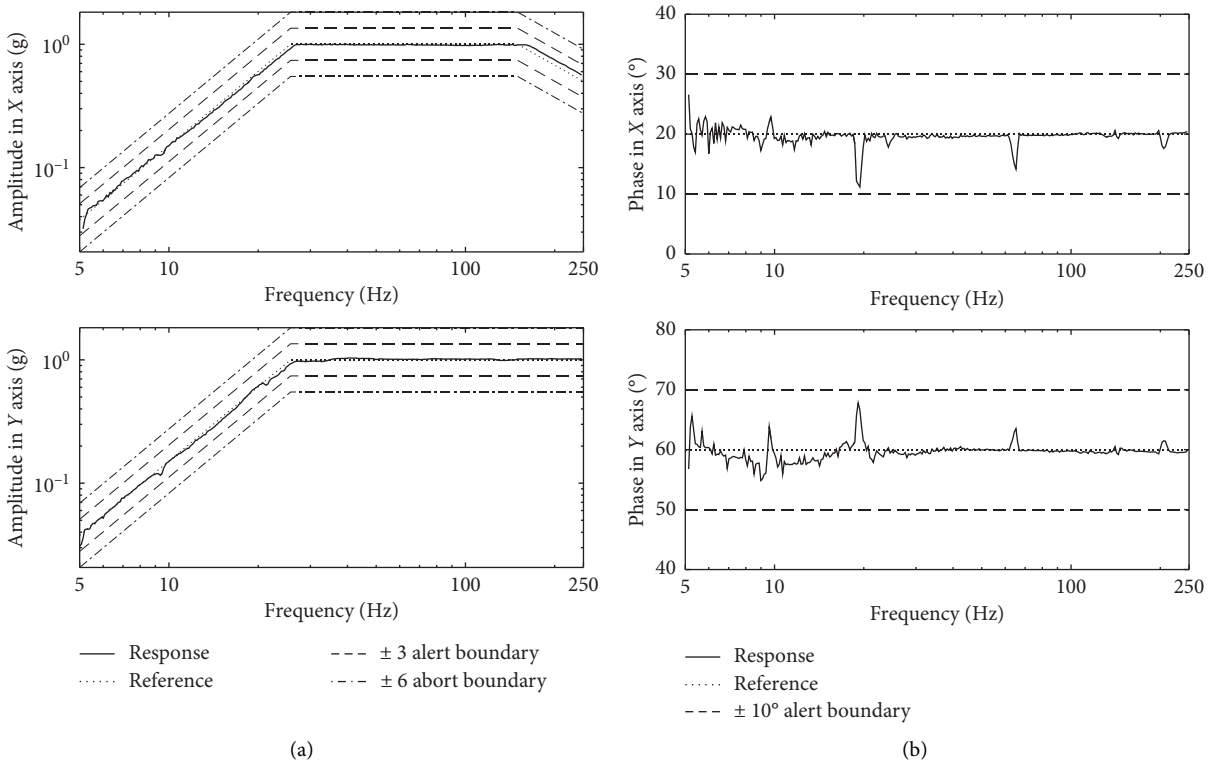

Figure 13: Responses of the normal level test after control.

the phases have some obtrusive deviations without control. In Figure 12, it is clear that after control both the amplitudes and phases are within the acceptable limits. From Figure 13, it can be seen that after the normal level is applied, the response spectra become slightly worse, but they are still within the alert limits.

5. Conclusion

An inverse multistep prediction model to represent the inverse system for the generation of drive signals for the MIMO continuous swept-sine test is proposed in the paper. The $\overline{T}$ matrix in the inverse multistep prediction model is truncated, thus causing the model to be noncausal and able to generate more stable drive signals. Since the length of the generated drive signals is less than the length of the input reference signals, the reference signals are used in an overlapped manner. In addition, in order to prevent the sudden occurrence of large drive damage to the test pieces and other test equipment, a transition section is added to the starting part of the reference signal; an offline control method is proposed in which the reference signals are modified by multiplication, and the drive signals are then updated using the inverse multistep prediction model.

A numerical example of a MIMO continuous swept-sine test on a cantilever beam is put forward, and the results show that the proposed method can perform excellently if the inverse multistep prediction model can be obtained precisely. The method is also verified by a MIMO continuous swept-sine test on a 3-axis shaker. The test results show that the response spectra can be controlled within the acceptable limits.

Data Availability

The test data used to support the findings of this study are available from the corresponding author upon request.

Disclosure

This study was performed in the State Key Laboratory of Mechanics and Control of Mechanical Structures.

Conflicts of Interest

The authors declare that they have no conflicts of interest.

Acknowledgments

This project was funded by the Priority Academic Program Development of Jiangsu Higher Education Institutions.

References

[1] C. Braccesi, F. Cianetti, L. Goracci, and M. Palmieri, "Sine-Sweep qualification test for engine components: the choice of simulation technique," *Procedia Structural Integrity*, vol. 24, pp. 360–369, 2020.

[2] MIL-STD-810G_CHG-1 Department of Defense Test Method Standard for Environmental Engineering Considerations and Laboratory Tests, 2014.

[3] A. Angeli, B. Cornelis, and M. Troncossi, "Synthesis of Sine-on-Random vibration profiles for accelerated life tests based on fatigue damage spectrum equivalence," *Mechanical Systems and Signal Processing*, vol. 103, pp. 340–351, 2018.

[4] C. J. Kim, "Accelerated sine-on-random vibration test method of ground vehicle components over conventional single mode excitation," *Applied Sciences*, vol. 7, no. 8, p. 805, 2017.

[5] K. Napolitano and D. Linehan, "Multiple sine sweep excitation for ground vibration tests," in *Proceedings of the the 27th Conference and Exposition on Structural Dynamics*, Oriando, Florida USA, 2009.

[6] M. A. Underwood, *Adaptive Control Method for Multiexciter Sine Tests*, 1994.

[7] M. A. Underwood and T. Keller, "Recent system development for multi-actuator vibration control," *Sound Vibration*, vol. 35, pp. 16–23, 2001.

[8] M. A. Underwood, "Multi-exciter testing applications: theory and practice," in *Proceedings-Institute of Environmental Sciences and Technology*, Anaheim, CA, USA, pp. 12–15, 2002.

[9] G. Gloth and M. Sinapius, "Analysis of swept-sine runs during modal identification," *Mechanical Systems and Signal Processing*, vol. 18, no. 6, pp. 1421–1441, 2004.

[10] B. Y. Zhang, H. H. Chen, and X. D. He, "New control method for MIMO swept-sine test," *Journal of Vibration and Shock*, vol. 34, pp. 198–202, 2015, in Chinese.

[11] A. G. Piersol, T. L. Paez, and C. M. Harris, *Harris' Shock and Vibration Handbook*, McGraw-Hill, New York, NY, USA, 2010.

[12] L. Yin, L. Zhang, D. Cong, and J. Han, "Sine swept vibration control based on offline iteration technique," in *International Conference on Intelligent Human-Machine Systems and Cybernetics*, pp. 456–461, Hangzhou, China, 2013.

[13] D. C. Kammer and A. D. Steltzner, "Structural identification using inverse system dynamics," *Journal of Guidance, Control, and Dynamics*, vol. 23, no. 5, pp. 819–825, 2000.

[14] D. C. Kammer and A. D. Steltzner, "Structural identification of mir using inverse system dynamics and mir/shuttle docking data," *Journal of Vibration and Acoustics*, vol. 123, no. 2, pp. 230–237, 2000.

[15] M. Allen and T. Carne, "Comparison of inverse structural filter (ISF) and sum of weighted accelerations (SWAT) time domain force identification methods," in *Proceedings of the the 47th AIAA/ASME/ASCE/AHS/ASC Structures, Structural Dynamics, and Materials Conference*, Newport, Rhode Island, 2006.

[16] M. S. Allen and T. G. Carne, "Delayed, multi-step inverse structural filter for robust force identification," *Mechanical Systems and Signal Processing*, vol. 22, no. 5, pp. 1036–1054, 2008.

[17] Y. M. Mao, X. L. Guo, and Y. Zhao, "A state space force identification method based on Markov parameters precise computation and regularization technique," *Journal of Sound and Vibration*, vol. 329, no. 15, pp. 3008–3019, 2010.

[18] H. Chen, P. Wang, and J. Sun, "Generation of multi-input multi-output non-Gaussian driving signal based on inverse system method," *Acta Astronautica*, vol. 37, pp. 1544–1551, 2016.

[19] R. Zheng, H. Chen, and X. He, "Control method for multiple-input multiple-output non-gaussian random vibration test," *Packaging Technology and Science*, vol. 30, no. 7, pp. 331–345, 2017.

[20] R. Zheng, H. Chen, D. Vandepitte, and Z. Luo, "Multi-exciter stationary non-Gaussian random vibration test with time domain randomization," *Mechanical Systems and Signal Processing*, vol. 122, pp. 103–116, 2019.

[21] J.-N. Juang and M. Phan, *Identification and Control of Mechanical Systems*, Cambridge University Press, Cambridge, UK, 2001.

[22] Z. Wu, S. Bian, C. Xiang, and Y. Tong, *A New Method for TSVD Regularization Truncated Parameter Selection*, Mathematical Problems in Engineering, vol. 2013, Article ID. 161834, 9 pages, 2013.

[23] X. Cui, H. Chen, X. He, and S. Jiang, "Matrix power control algorithm for multi-input multi-output random vibration test," *Chinese Journal of Aeronautics*, vol. 24, no. 6, pp. 741–748, 2011.

[24] M. Feldman, "Hilbert transform in vibration analysis," *Mechanical Systems and Signal Processing*, vol. 25, no. 3, pp. 735–802, 2011.